Investigation of Thermoelectric Properties of $CH_3NH_3PbI_3$: Density Functional Theory and Boltzmann Transport Calculations

Ibrahim Omer Abdallah[1,2], Daniel P Joubert[1], and Mohammed S H Suleiman[1,3]

[1] The National Institute for Theoretical Physics, School of Physics and Mandelstam Institute for Theoretical Physics, University of the Witwatersrand, Johannesburg, Wits 2050, South Africa.
[2] Department of Scientific Laboratories, Sudan University of Science and Technology, Khartoum, Sudan.
[3] Department of Basic Sciences, Imam Abdulrahman Bin Faisal University, P. O. Box 1982, Dammam, KSA.

E-mail: ibraphysics@gmail.com

Abstract. Mixed organometal perovskite $CH_3NH_3PbI_3$ has recently emerged as a promising candidate for low cost, high-efficiency solar cells. The materials' thermoelectric properties which are key to the solar thermoelectric applications have not been investigated extensively. In this paper, the thermoelectric properties of organic-inorganic halide perovskite $CH_3NH_3PbI_3$ were studied by solving the semiclassical Boltzmann transport equation on top of density functional theory (DFT) calculations using maximally-localised Wannier functions (MLWFs). Electronic transport properties were evaluated within the constant relaxation time approximation at different temperatures: 50 K, 100 K and 150 K. The Seebeck coefficient (S), electrical conductivity (σ), electronic thermal conductivity (κ_e), power factor ($S^2\sigma$) and figure of merit (ZT) as function of chemical potential are analysed. The maximal figure of merit is found to be 0.06 and 0.122 at 100 K and 150 K, respectively.

1. Introduction

Organic-inorganic perovskites ABI_3 (A = CH_3NH_3 or NH_2CHNH_2; B = Sn, Pb), have been specified as light harvesting materials [1]. In addition, they were treated as new thermoelectric materials with a large Seebeck coefficient and low thermal conductivity [2, 3], implying that these materials might be potential candidates for thermoelectric applications [4]. The efficiency of thermoelectric devices is characterized by a dimensionless figure of merit ZT[1] $= S^2\sigma T/\kappa$, where S, σ, T and κ are Seebeck coefficient, electrical conductivity, temperature and total thermal conductivity, respectively [6]. Both phonons and electrons are heat carriers, therefore the total thermal conductivity has two contributions, the lattice thermal conductivity component κ_l and the electronic thermal conductivity component κ_e. Thermoelectric materials with a large thermoelectric figure of merit can convert heat to electricity via the Seebeck effect. To have a

[1] "The expressions for figure of merit , Z and ZT, are used interchangeably in the field of TE. Z is the figure of merit with units of 1/K (1/T), and ZT is the standard notation for the dimensionless figure of merit" [5].

large figure of merit one needs a large power factor $S^2\sigma$ and low thermal conductivity κ. In the present work, we studied the thermoelectric properties of the $CH_3NH_3PbI_3$ in an orthorhombic system from a combination of semiclassical Boltzmann transport equation and density functional theory calculations using maximally-localised Wannier functions (MLWFs). $CH_3NH_3PbI_3$ is orthorhombic at low temperature (space group Pnma, 62), with the unit cell shown in Figure 1. Section 2 describes the methodology used in the investigation. Section 3 presents the results and discussion. Finally, we shall give our conclusion in section 4.

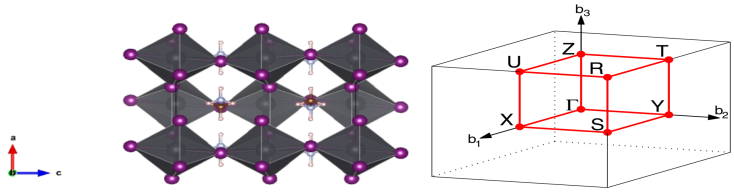

Figure 1. (Color online) The crystal structure of orthorhombic $CH_3NH_3PbI_3$ (left) and its corresponding Brillouin zone (right). Filled red circles are the high symmetry points, while the red bold lines indicate segments of the high symmetry path ($\Gamma - X - S - Y - \Gamma$).

2. Methodology

In this work, the investigation of the electronic structure properties was performed using the Vienna Ab-initio Simulation Package (VASP) [7, 8] based on Density Functional Theory (DFT) [9, 10]. The Projector-Augmented Wave (PAW) [11] method was employed to treat electron-ion interactions. To describe the electrons' exchange and correlation effects, we used the Generalized Gradient Approximation (GGA) as parametrized and revised by Perdew, Burke and Ernzerhof (PBEsol) [12]. $4 \times 4 \times 2$ Monkhorst-Pack meshes were used in sampling the Brillouin zone with an energy cut-off of 520 eV. The atomic positions were fully optimized until all components of the forces were less than 1 meV/atom.

The thermoelectric and electronic transport properties were calculated by solving the semiclassical Boltzmann transport equations in the constant relaxation-time approximation (here $\tau = 10^{-14}$ s) as implemented in the BoltzWann code [13]. The code uses a maximally-localized Wannier functions (MLWFs) [14] basis set to interpolate the bandstructure obtained from the above-mentioned DFT calculations. After using $6 \times 4 \times 4$ k-points for the construction of the MLWFs, a $40 \times 40 \times 40$ was utilized to calculate the electronic transport properties such as Seebeck coefficient S, electrical conductivity σ, electronic thermal conductivity κ_e and the power factor $S^2\sigma$. The computation of MLWFs has been performed within WANNIER90 package [15].

3. Results and discussion

3.1. Bandstructure and density of states

The bandstructure of the structurally optimized $CH_3NH_3PbI_3$ was calculated along the high symmetry points of the Brillouin zone (BZ) using the generalized gradient approximation (GGA) for solids (PBEsol). The calculated electronic bandstructure of $CH_3NH_3PbI_3$ is shown in Figure 2, together with total (TDOS) and projected (PDOS) density of states. Both the valence band maximum (VBM) and conduction band minimum (CBM) were found to be located at the Γ point of the Brillouin zone (BZ), hence the investigated material has a direct band-gap semiconductor character at the gamma Γ point. The calculated band gap according to PBEsol without including spin orbit coupling was found to be 1.57 eV in good agreement with the experimental result of 1.61 eV [16] and with other theoretical predictions [17, 18, 19]. Density of states around the fundamental band gap show that, only iodine I and lead Pb contribute to the DOS.

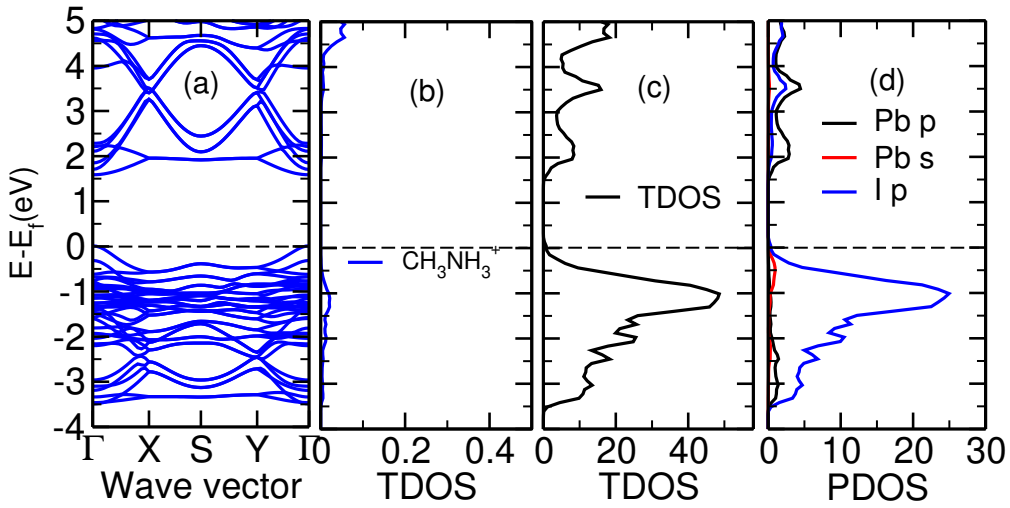

Figure 2. (Color online) DFT calculated electronic structure for $CH_3NH_3PbI_3$: (a) band structure; (b) $CH_3NH_3^+$ (TDOS); (c) total density of states (TDOS), (d) partial density of states (PDOS) (arb. units) using PBEsol.

3.2. Thermoelectric properties

The calculated properties are plotted in Figures 3-7 as functions of the chemical potential μ at temperatures: 50 K, 100 K and 150 K.

The Seebeck coefficient S, is defined as the ratio of the electric field to the temperature gradient when the electrical current is zero. The calculated Seebeck coefficients as a function of chemical potential μ at different temperatures are presented in Figure 3. It is clear that Seebeck coefficient of $CH_3NH_3PbI_3$ has positive values at chemical potential $\mu = 0$, indicating that it is a p-type semiconductor. In the z-direction the maximum values of the Seebeck coefficient S almost remained constant from 50 to 150 K.

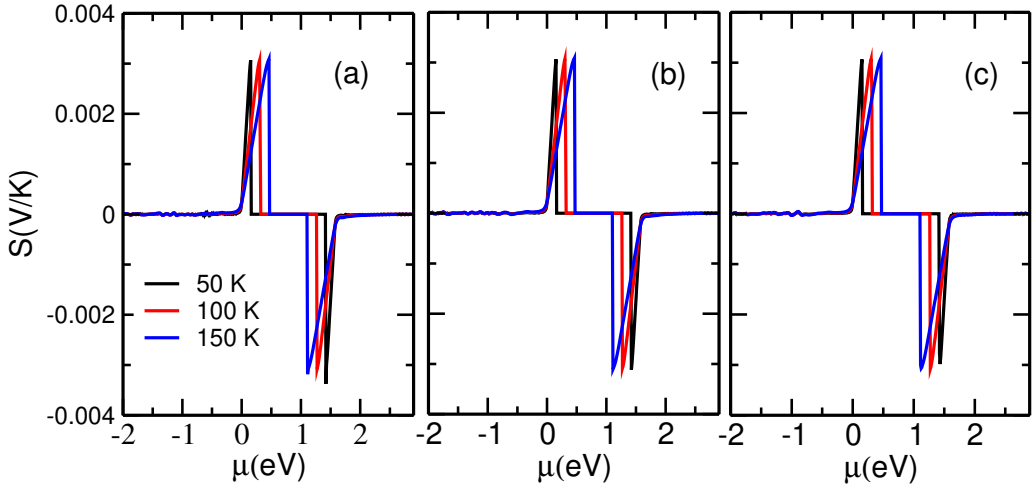

Figure 3. (Color online) Variation of Seebeck coefficient with respect to chemical potential at different temperatures in the (a) x-direction, (b) y-direction, and (c) z-direction.

The calculated electrical conductivity σ as a function of chemical potential at different temperatures are presented in Figure 4. Electrical conductivity was found to be almost

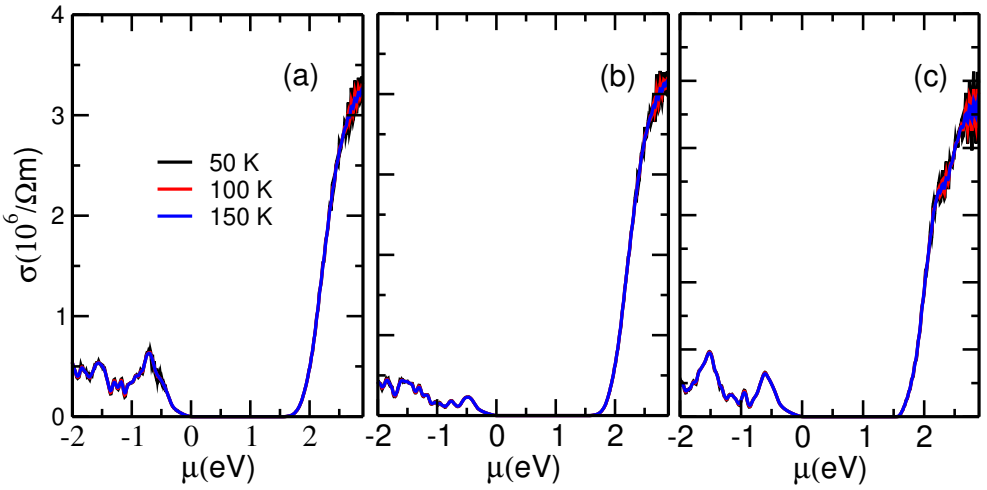

Figure 4. (Color online) Variation of electrical conductivity with respect to chemical potential at different temperatures in the (a) x-direction, (b) y-direction, and (c) z-direction.

temperature independent in the considered temperature range. This trend was observed in SnSe [20] and ScRhTe [21]. In general, the value of electrical conductivity increases with increase in absolute value of the chemical potential at all temperatures with the highest value 4.58×10^6 $\Omega^{-1}\mathrm{m}^{-1}$ in the z-direction at chemical potential 2.84 eV.

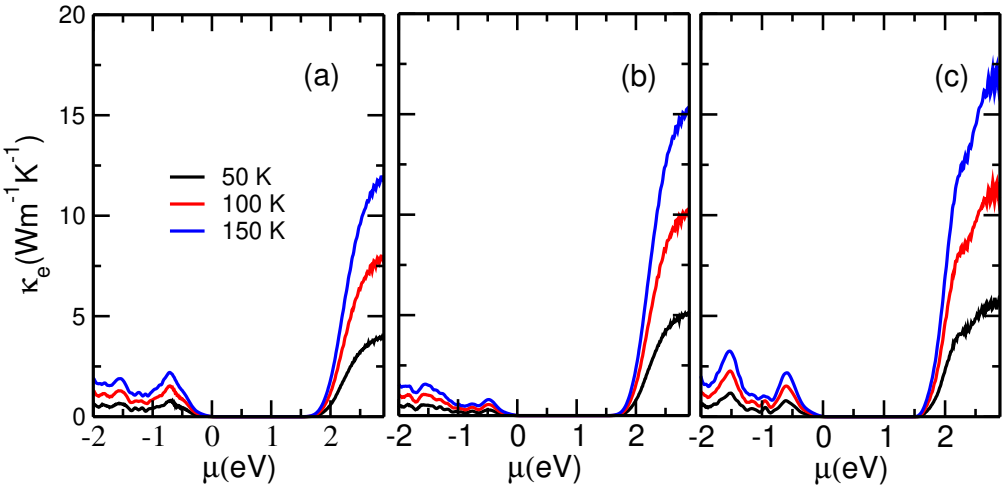

Figure 5. (Color online) Electronic thermal conductivity as a function of chemical potential at different temperatures in the (a) x-direction, (b) y-direction, and (c) z-direction.

The electronic thermal conductivity κ_e as a function of chemical potential at different temperatures are plotted in Figure 5. At chemical potential 2.84 eV the maxima of the electronic thermal conductivity in z-direction increases from 5.8 $\mathrm{Wm}^{-1}\mathrm{K}^{-1}$ at 50 K to 17.3 $\mathrm{Wm}^{-1}\mathrm{K}^{-1}$ at 150 K.

The power factor $S^2\sigma$ as a function of chemical potential at different temperatures is shown in Figure 6. At chemical potential 1.96 eV, the maximum calculated value of the power factor was found to be 0.00042 $\mathrm{Wm}^{-1}\mathrm{K}^{-2}$ and 0.00072 $\mathrm{Wm}^{-1}\mathrm{K}^{-2}$ in z-direction at 100 K and 150 K, respectively.

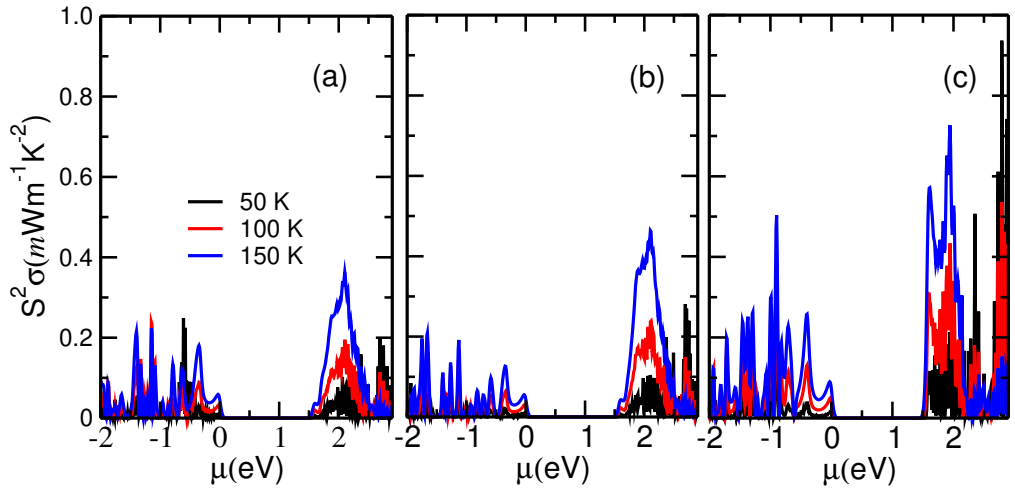

Figure 6. (Color online) Calculated power factor as a function of chemical potential at different temperatures in the (a) x-direction, (b) y-direction, and (c) z-direction.

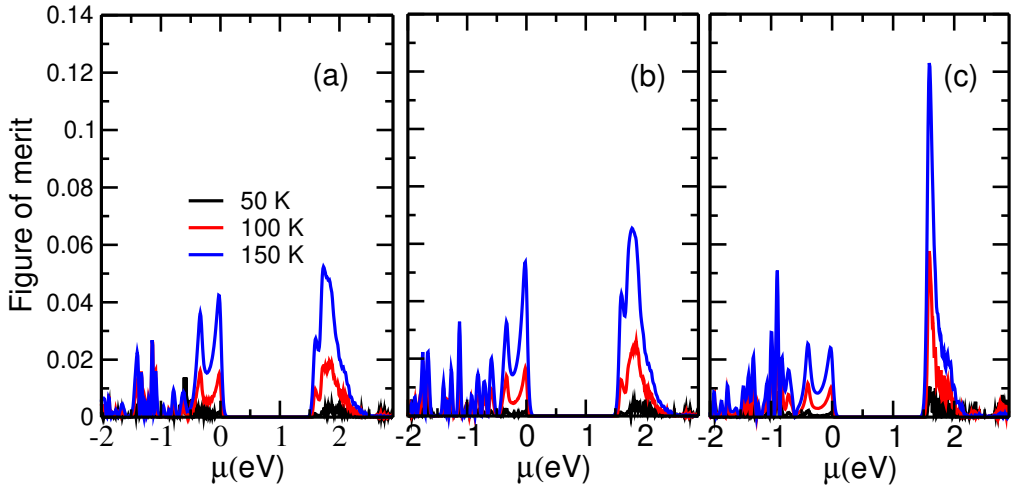

Figure 7. (Color online) Calculated figure of merit as a function of chemical potential at different temperatures in the (a) x-direction, (b) y-direction, and (c) z-direction.

Using the calculated transport coefficients, and the calculated lattice thermal conductivities K_L from Ref. [22], the figure of merit as a function of chemical potential at low temperatures along x-, y- and z-directions is obtained as shown in Figure 7. We can see that the values of ZT increase with increasing temperature. The maxima of the ZT in the z-direction increases from 0.06 at 100 K to 0.122 at 150 K.

From the presented figures, it is evident that the obtained Seebeck coefficient (Figure 3) and figure of merit (Figure 7) are nearly isotropic; while the electrical conductivity (Figure 4), the electronic thermal conductivity (Figure 5), and the power factor (Figure 6) are highly anisotropic with their optimal values in the z-direction.

4. Conclusion

We have carried out a detailed theoretical study of the thermoelectric properties of $CH_3NH_3PbI_3$ in an orthorhombic system for the first time based on density functional theory combined

with the Boltzmann transport theory within the constant relaxation time approximation as implemented in BoltzWann code. Based on the results, we show that the optimum ZT values of the orthorhombic $CH_3NH_3PbI_3$ was found to be 0.06 at 100 K and 0.122 at 150 K in the z direction.

Acknowledgements
IOAA would like to acknowledge the support he received from NRF-TWAS for funding, and Sudan University of Science and Technology (SUST). We also wish to acknowledge the Centre for High Performance Computing (CHPC), South Africa, for providing us with computing facilities.

References

[1] Lee C, Hong J, Stroppa A, Whangbo M H and Shim J H 2015 *RSC Advances* **5** 78701–78707
[2] Stoumpos C C, Malliakas C D and Kanatzidis M G 2013 *Inorganic chemistry* **52** 9019–9038
[3] Pisoni A, Jaćimović J, Barišić O S, Spina M, Gaál R, Forró L and Horváth E 2014 *arXiv preprint arXiv:1407.4931*
[4] He Y and Galli G 2014 *Chemistry of Materials* **26** 5394–5400
[5] Tritt T M and Subramanian M 2006 *MRS bulletin* **31** 188–198
[6] Goldsmid H, Nolas G and Sharp J 2001 Thermoelectrics: Basic principles and new materials developments
[7] Kresse G and Hafner J 1993 *Physical Review B* **47** 558
[8] Kresse G and Hafner J 1994 *Physical Review B* **49** 14251
[9] Hohenberg P and Kohn W 1964 *Physical review* **136** B864
[10] Kohn W and Sham L J 1965 *Physical review* **140** A1133
[11] Kresse G and Joubert D 1999 *Physical Review B* **59** 1758
[12] Perdew J P, Ruzsinszky A, Csonka G I, Vydrov O A, Scuseria G E, Constantin L A, Zhou X and Burke K 2008 *Physical Review Letters* **100** 136406
[13] Pizzi G, Volja D, Kozinsky B, Fornari M and Marzari N 2014 *Computer Physics Communications* **185** 422–429
[14] Souza I, Marzari N and Vanderbilt D 2001 *Physical Review B* **65** 035109
[15] Mostofi A A, Yates J R, Lee Y S, Souza I, Vanderbilt D and Marzari N 2008 *Computer physics communications* **178** 685–699
[16] Baikie T, Fang Y, Kadro J M, Schreyer M, Wei F, Mhaisalkar S G, Graetzel M and White T J 2013 *Journal of Materials Chemistry A* **1** 5628–5641
[17] Wang Y, Gould T, Dobson J F, Zhang H, Yang H, Yao X and Zhao H 2013 *Physical Chemistry Chemical Physics* **16** 1424–1429
[18] Brivio F, Frost J M, Skelton J M, Jackson A J, Weber O J, Weller M T, Goni A R, Leguy A M, Barnes P R and Walsh A 2015 *Physical Review B* **92** 144308
[19] Ali I O A, Joubert D P and Suleiman M S H 2018 *Materials Today: Proceedings* **5** 10570–10576
[20] Wang F Q, Zhang S, Yu J and Wang Q 2015 *Nanoscale* **7** 15962–15970
[21] Kaur K and Kaur J 2017 *Journal of Alloys and Compounds* **715** 297–303
[22] Ali I O A, Joubert D P and Suleiman M S H 2018 *The European Physical Journal B* **91** 263 ISSN 1434-6036